The microtubule-binding protein CLIP-170 coordinates mDia1 and actin reorganization during CR3-mediated phagocytosis

Elodie Lewkowicz,[1,2] Floriane Herit,[1,2] Christophe Le Clainche,[3] Pierre Bourdoncle,[1,2] Franck Perez,[4,5] and Florence Niedergang[1,2]

[1]Institut Cochin, Université Paris Descartes, Centre National de la Recherche Scientifique, Unité Mixte de Recherche 8104, 75014 Paris, France
[2]Institut national de la santé et de la recherche médicale, Unité 567, 75014 Paris, France
[3]Centre National de la Recherche Scientifique, Unité Propre de Recherche 3082, 91190 Gif-sur-Yvette, France
[4]Institut Curie, Centre de Recherche, 75248 Paris, France
[5]Centre National de la Recherche Scientifique, Unité Mixte de Recherche 144, 75248 Paris, France

Microtubule dynamics are modulated by regulatory proteins that bind to their plus ends (+TIPs [plus end tracking proteins]), such as cytoplasmic linker protein 170 (CLIP-170) or end-binding protein 1 (EB1). We investigated the role of +TIPs during phagocytosis in macrophages. Using RNA interference and dominant-negative approaches, we show that CLIP-170 is specifically required for efficient phagocytosis triggered by αMβ2 integrin/complement receptor activation. This property is not observed for EB1 and EB3. Accordingly, whereas CLIP-170 is dynamically enriched at the site of phagocytosis, EB1 is not. Furthermore, we observe that CLIP-170 controls the recruitment of the formin mDia1, an actin-nucleating protein, at the onset of phagocytosis and thereby controls actin polymerization events that are essential for phagocytosis. CLIP-170 directly interacts with the formin homology 2 domain of mDia1. The interaction between CLIP-170 and mDia1 is negatively regulated during αMβ2-mediated phagocytosis. Our results unravel a new microtubule/actin cooperation that involves CLIP-170 and mDia1 and that functions downstream of αMβ2 integrins.

Introduction

Microtubules are dynamic and asymmetrical elements of the cytoskeleton essential for cell organization. Their slowly polymerizing minus ends are generally attached to the microtubule-organizing center, whereas their plus ends explore the cell periphery. Microtubule plus ends display a dynamically unstable behavior (Mitchison and Kirschner, 1984): they alternate between growing and shrinking phases separated by pauses, catastrophes, and rescues in an apparently stochastic manner (Howard and Hyman, 2003; Karsenti et al., 2006). In vivo, microtubule dynamics are modulated by interacting proteins, including proteins that specifically bind to their plus ends (plus end tracking proteins or +TIPs) (Galjart and Perez, 2003; Galjart, 2005; Lansbergen and Akhmanova, 2006). The prototype +TIP is the cytoplasmic linker protein 170 (CLIP-170/CLIP-1/Bik1p/Tip1), which binds to polymerizing microtubules (Perez et al., 1999) and promotes their rescue (Komarova et al., 2002). A close relative of CLIP-170, CLIP-115/CLIP-2, is expressed in many mammalian cells and contributes to CLIP activity (De Zeeuw et al., 1997; Hoogenraad et al., 2000; Lansbergen et al., 2004). End-binding protein 1 (EB1; Bim1p/Mal3) also binds to microtubule plus ends and was recently proposed to serve as a platform for other +TIPs such as CLIP-170, but also for the dynactin component p150^{Glued}, CLASP, or MCAK (Akhmanova and Steinmetz, 2008). +TIPs stabilize microtubules at the cell cortex and thereby guide them to specific locations; this is thought to be critical for cell polarity, cell division, and cell migration (Galjart, 2005). However, although CLIP-170 was initially identified as a linker between endosomes and microtubules (Pierre et al., 1992), the involvement of CLIP-170 in secretory or endocytic trafficking events has not been extensively studied. We decided to study the role of +TIPs in phagocytosis, a cytoskeleton-dependent

Correspondence to Florence Niedergang: florence.niedergang@inserm.fr

Abbreviations used in this paper: CLIP, cytoplasmic linker protein; CR3, complement receptor 3; DAD, diaphanous autoregulatory domain; EB, end-binding protein; FcR, Fc receptor; FH2, formin homology 2; shRNA, small hairpin RNA; SRBC, sheep red blood cell.

The Rockefeller University Press $30.00
J. Cell Biol. Vol. 183 No. 7 1287–1298
www.jcb.org/cgi/doi/10.1083/jcb.200807023

pathway used by specialized cells of the immune system to internalize and degrade microorganisms, apoptotic bodies, and particulate antigens (Aderem and Underhill, 1999; Stuart and Ezekowitz, 2005).

Phagocytosis is initiated by the triggering of surface phagocytic receptors such as receptors for immunoglobulins (Fc receptor [FcR]) or for complement (e.g., complement receptor 3 [CR3]), two proteins that opsonize the particulate antigen. Signaling pathways downstream of these receptors differ, although they both induce the polymerization of actin, which is a prerequisite to phagocytosis (Aderem and Underhill, 1999; Niedergang and Chavrier, 2005; Stuart and Ezekowitz, 2005). Signaling downstream of the FcR involves the clustering of Src family tyrosine kinases and the activation of Rac1 and Cdc42 GTP-binding proteins. This, in turn, stimulates the actin-nucleating activity of the Arp2/3 complex (Niedergang and Chavrier, 2005). The CR3 complement receptor is an integrin (CD11b/CD18 [αMβ2]) that requires activation by an "inside out" signal (Dupuy and Caron, 2008) provided by cytokines or mimicked experimentally by phorbol esters. The inside out signaling relies on the small GTP-binding protein Rap1 and the actin-binding protein talin (Caron, 2003; Lim et al., 2007). Clustering of CR3 induces the activation of RhoA and the recruitment of downstream effectors (Dupuy and Caron, 2008). The Rho kinase (ROCK) and its target Myosin II have been implicated in the accumulation of the actin-nucleating Arp2/3 complex and F-actin assembly (Olazabal et al., 2002). In addition, the RhoA effector mDia1, which is a member of the formin family of actin nucleators (Evangelista et al., 2003; Wallar and Alberts, 2003), is recruited and required for efficient CR3-mediated phagocytosis (Olazabal et al., 2002; Colucci-Guyon et al., 2005).

Although the importance of actin during phagosome formation is well established, the contribution of microtubules has not been extensively studied (Harrison and Grinstein, 2002). Here we analyzed the specific role of microtubule-binding proteins during CR3-mediated phagocytosis. We show that CLIP-170, but not EB1, is targeted to phagocytic cups and is required for efficient CR3-mediated phagocytosis. In addition, we found that CLIP-170 is important for the recruitment of mDia1 at phagocytic sites and for optimal actin polymerization, thus identifying a crucial cross talk between microtubules and actin.

Results

CLIP-170–labeled microtubule plus ends are enriched at sites of CR3-mediated phagocytosis

We first set out to study the dynamics of microtubules during phagocytosis. For this, we either labeled microtubule plus ends by immunofluorescence using an anti–CLIP-170 antibody or expressed a YFP–CLIP-170 construct transiently in RAW264.7 cells. As in other cells (Perez et al., 1999; Komarova et al., 2002), CLIP-170 labeling appears as cometlike structures at the plus ends of microtubules (Fig. 1 A and Fig. 2 A). We followed YFP–CLIP-170 comet movement in resting cells using a tracking software. Although the majority of the comets arose from the microtubule-organizing center and moved toward the periphery, some comets seemed to be generated at a more distal site. The mean speed measured was 0.3 ± 0.016 μm/s (n = 1360 comets), which is in agreement with the speed measured in other cell types (Perez et al., 1999; unpublished data).

We then focused on CR3-mediated phagocytosis because, as described previously (Newman et al., 1991; Allen and Aderem, 1996), we observed that taxol treatment, which stabilizes microtubules, decreased the efficiency of CR3-mediated phagocytosis to 32 ± 5% of control cells. In contrast, FcR-mediated phagocytosis or zymosan uptake were less affected (72 ± 10 and 82 ± 13% of control cells, respectively; Fig. S1 A, available at http://www.jcb.org/cgi/content/full/jcb.200807023/DC1). We allowed macrophages to interact with complement-opsonized sheep red blood cells (SRBCs) for 10 min at 37°C to target phagocytosis by CR3. Macrophages were then fixed and stained to detect endogenous CLIP-170 as well as F-actin (Fig. S1 B). We observed that CLIP-170 was present, although not strongly accumulated, in phagocytic cups together with polymerized actin. Microtubules were also present at the site of phagocytosis (Fig. S1 C). Because actin polymerization is a rapid and transient event concomitant to phagosome formation (Swanson et al., 1999; Coppolino et al., 2002; Araki et al., 2003; Henry et al., 2004), this suggested that CLIP-170 is recruited early during phagosome formation induced by CR3 clustering.

To better analyze the effect of phagocytosis on the dynamics of the microtubule plus ends, we tracked the cometlike structures in phagocytosing macrophages (Fig. 1, B and C). We defined regions of interest undergoing phagocytosis to compare them with the rest of the cell. The mean speed measured was similar in the area undergoing phagocytosis to resting area (unpublished data). In contrast, the number of comets in a phagocytosing area was more than two times higher than in nonphagocytosing areas (2.4 ± 0.5; Fig. 1 F). To verify whether this observation was specific to phagocytosis, we performed a similar analysis in cells treated with macrophage colony-stimulating factor to induce ruffling and the formation of actin-rich regions (Fig. 1, D and E). The number of comets in regions of actin activity was not different from the number calculated in regions devoid of actin activity.

Together, these results show that CLIP-170, which highlights polymerizing microtubule plus ends, is accumulated at sites of phagocytosis, but not in other regions of actin polymerization activity. This indicates that, compared with resting regions of macrophages, microtubule growth is promoted in these areas.

CLIP-170 is necessary for efficient CR3-mediated phagocytosis

Next we assessed whether CLIP-170 was required for CR3-mediated phagocytosis in macrophages (Fig. 2). Because RAW264.7 macrophages express both CLIP-170 and CLIP-115, we first inactivated their function by overexpressing a dominant-negative mutant of CLIP-170 that lacks the microtubule-binding domain (CLIP-170ΔH) and that was reported to delocalize endogenous CLIP-170 and CLIP-115 from the plus ends of microtubules (Fig. 2 A; Komarova et al., 2002). Expression of GFP–CLIP-170ΔH in RAW264.7 macrophages led to a 41 ± 4%

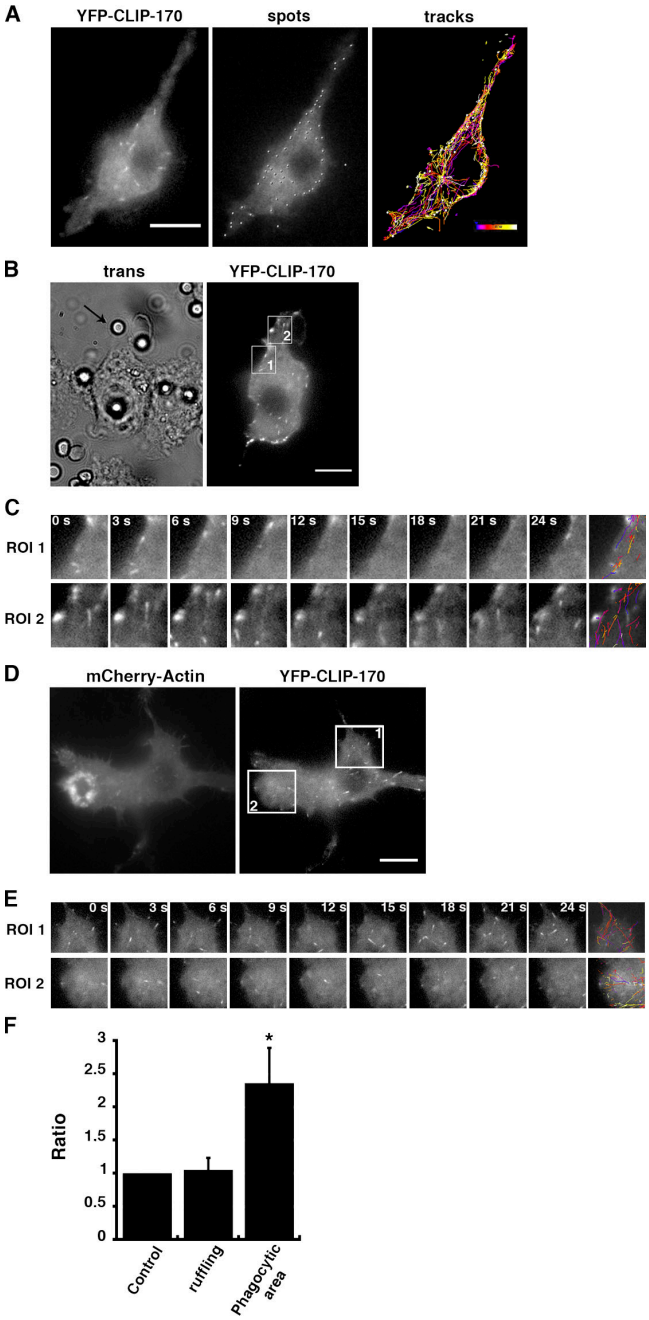

Figure 1. **CLIP-170 is recruited at sites of phagocytosis.** (A) Dynamics of CLIP-170–positive comets at steady-state in macrophages. Cells were transfected with pYFP–CLIP-170 and 24 h later time-lapse imaging was performed (left). Tracking of CLIP-170–positive structures was performed using Imaris 5.7 software (spots corresponding to CLIP-170–positive structures [middle] and tracks followed during 150 s [right]). Colored bar, time scale. Bar, 10 µm. (B) Dynamics of CLIP-170 in phagocytosing macrophages. RAW264.7 macrophages were incubated at 37°C with C3bi-SRBCs and observed by wide-field fluorescence microscopy. Transmission (left) and fluorescence (right) images were recorded every second during 150 s. Transmission acquisition shows phagocytosis of an opsonized SRBC (left, arrow). The cell was divided in two regions of interest (ROI1 and ROI2). ROI1 corresponds to a nonphagocytosing area, whereas ROI2 is a phagocytosing area. Bar, 10 µm. (C) Time stack of images acquired in ROI1 and ROI2 as described in B. The last image shows the tracks followed during 150 s. (D) Dynamics of CLIP-170 in RAW264.7 macrophages treated with macrophage colony-stimulating factor to induce ruffling and spreading. Cells were transfected with pYFP–CLIP-170 and pmCherry-actin and 24 h later time-lapse imaging was performed as in A. mCherry-actin (left) and YFP–CLIP-170 (right) images were recorded every second during 150 s. The cell was divided into an area with actin activity (ROI2) and a resting area (ROI1). Bar, 10 µm. (E) Time stack of images acquired in ROI1 and ROI2 as described in D. Selected images are shown. The last image shows the tracks followed during 150 s. (F) Cells were analyzed as described in B and D. The number of comets per surface unit was calculated for regions of interest in different cells and the ratio between phagocytic and nonphagocytic (control) areas or between areas with actin activity (ruffling) and resting areas (control) was measured. The means ± SEM of 2,026 comets (in 7 phagocytosing cells) and the means ± SEM of 13,285 comets (in 11 cells with ruffles) are plotted. *, $P < 0.05$.

decrease in CR3-mediated phagocytosis efficiency compared with control conditions, whereas association of the opsonized SRBCs was not affected (Fig. 2 B).

We then used RNA interference to knock down the expression of the protein by transfecting RAW264.7 macrophages with pSUPER plasmids encoding small hairpin RNA (shRNA) against CLIP-170 (pSUPER-170A), CLIP-115 (pSUPER-115A and pSUPER-115B), or CLIP-170 and CLIP-115 (pSUPER-AB; Lansbergen et al., 2004). We observed a diminished CLIP-170 or CLIP-115 expression in shRNA-treated cells compared with control cells treated with a nonspecific pSUPER plasmid (Fig. 2, C and D). The efficiency of particle binding and phagocytosis was monitored in CLIP-170– or CLIP-115–depleted cells identified by immunostaining with anti–CLIP-170 and –CLIP-115 antibodies. Although the association of particles was not decreased in CLIP-170–, CLIP-115–, or CLIP-170/115–depleted cells, internalization of complement-opsonized particles was reduced by 37 ± 0.4 and 47 ± 5% in CLIP-170 and CLIP-170/CLIP-115 shRNA-treated cells, respectively (Fig. 2 E). Of note, neither the mutant construct nor RNA interference treatments affected the efficiency of phagocytosis via the FcR (Fig. S2, available at http://www.jcb.org/cgi/content/full/jcb.200807023/DC1).

Therefore, using dominant-negative and RNA interference approaches, our data support a major role for CLIP-170 in efficient CR3-mediated phagocytosis.

EB1 is dispensable for phagocytosis and is not recruited in phagocytic cups, whereas CLIP-170 is

To address the specificity of the role of CLIP-170 in phagocytosis, we analyzed the recruitment and function of another +TIP during phagocytosis (Fig. 3). We chose EB1 because this protein was recently reported to associate directly with microtubule plus ends and to subsequently recruit CLIP-170 and $p150^{Glued}$ (Watson and Stephens, 2006). We inactivated EB1 expression with specific siRNA as reported (Wen et al., 2004). Although the depletion observed by Western blotting and immunofluorescence was more efficient than that observed for CLIP-170 (Fig. 3, A and B), it hardly affected the capacity of the cells to bind to or to phagocytose opsonized particles (Fig. 3 C). We also depleted the RAW264.7 macrophages of EB3, a +TIP protein closely related to EB1. The depletion of EB3 alone, or EB1 and EB3, did not significantly impair CR3-mediated phagocytosis.

We then checked whether depletion of CLIP-170 or EB1 had any effect on the expression and the localization of EB1 or

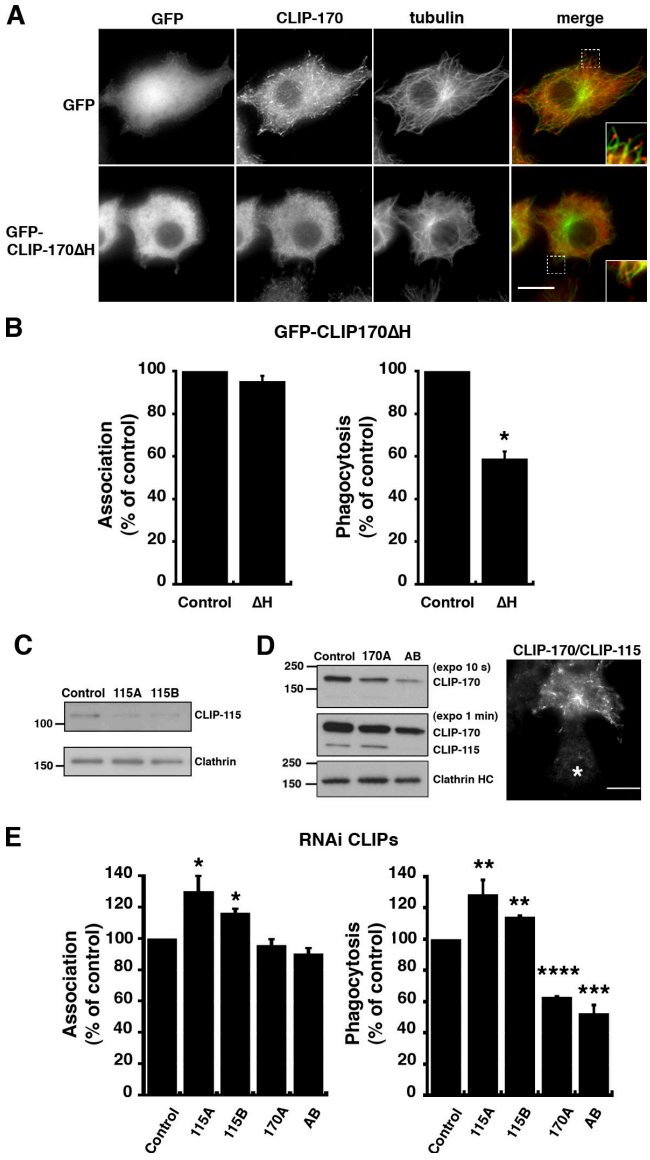

Figure 2. **CLIP-170 is important for CR3-mediated phagocytosis.** (A) RAW264.7 cells were transfected with pEGFP–CLIP-170ΔH, encoding a dominant-negative mutant of CLIP-170 (bottom) or with pEGFP as a control (top). After 24 h, macrophages were labeled with the anti–CLIP-170/CLIP-115 antibodies (#2221 serum) and with anti-tubulin antibodies, and then analyzed by wide-field fluorescence microscopy. Insets with magnified images are shown on the right. Bar, 10 µm. (B) A dominant-negative form of CLIP-170 inhibits CR3-mediated phagocytosis. Macrophages were transfected with pEGFP–CLIP-170ΔH or with pEGFP as a control. After 24 h, macrophages were allowed to phagocytose C3bi-SRBCs for 3 and 60 min at 37°C, and then fixed and stained with Cy3–anti-rabbit IgG antibodies to detect SRBCs. Efficiencies of association and phagocytosis were scored in 50 cells expressing GFP–CLIP-170ΔH and 50 GFP-expressing control cells. Results are expressed as a percentage of control cells. The means ± SEM of at least three independent experiments are plotted. *, $P < 0.0001$. (C) RAW264.7 macrophages were transfected with pSUPER-115A, pSUPER-115B, or pSUPER-G (directed against giantin) as a control. After 48 h, lysates were prepared and Western blotting was performed with anti–CLIP-170/115 antibodies (top) or with anti-clathrin (bottom) as a loading control. (D) RAW264.7 macrophages were transfected with pSUPER-170A (directed against CLIP-170), pSUPER-AB (directed against CLIP-170 and CLIP-115), or pSUPER-G (directed against giantin) as a control. After 48 h, lysates were prepared and Western blotting was performed with anti–CLIP-170/115 antibodies (10 s [top] or 1 min [middle] of film exposure) or with anti-clathrin (bottom). In addition, cells were fixed, permeabilized, and labeled with anti–CLIP-170/115 antibodies followed by Cy3–anti-rabbit IgG antibodies. Cells were analyzed by wide-field fluorescence microscopy (right). The image shows a cell depleted of CLIP-170/115 with pSUPER-AB (asterisk). Bar, 10 µm. (E) Depletion of CLIP-170 but not CLIP-115 inhibits phagocytosis. Macrophages were transfected as described in C and D, and then allowed to phagocytose C3bi-SRBCs for 3 and 60 min at 37°C and fixed and stained with Cy2–anti-rabbit IgG antibodies and, after permeabilization, with anti–CLIP-170 or anti–CLIP-115 antibodies. The efficiencies of association and phagocytosis were calculated for 50 CLIP-115–depleted cells (115A and 115B), 50 CLIP-170–depleted cells (170A), 50 CLIP-170/115–depleted cells (AB), and 50 control cells. Results are expressed as a percentage of control cells. The means ± SEM of three independent experiments are plotted. *, $P < 0.05$; **, $P < 0.005$; ***, $P < 0.001$; ****, $P < 0.0001$.

CLIP-170, respectively (Fig. S3, available at http://www.jcb.org/cgi/content/full/jcb.200807023/DC1). Depletion of EB1 did not affect the expression of CLIP-170 (Fig. S3 A) and had no apparent effect on the localization of this +TIP (Fig. S3 C). Similarly, depletion of CLIP-170 had no strong effect on the expression of EB1 (Fig. S3, B and D). These results confirm that the effects on phagocytosis observed when CLIP-170 function is impaired are specific to this +TIP.

To gain a better understanding of the functional difference we observed between CLIP-170 and EB1, we analyzed the localization of the two proteins in phagocytic cups as compared with resting macrophages. For this, macrophages were allowed to contact C3bi-SRBCs for 10 min and were fixed and stained with phalloidin, anti–CLIP-170, and anti-EB1 antibodies (Fig. 3, D and E). In resting and phagocytic cells, EB1 and CLIP-170 were often found colocalized in cometlike structures (in 62 ± 4 and 58 ± 5% of the cases, respectively). Interestingly, in phagocytic areas defined by F-actin cups, we observed a decrease in the number of structures labeled with EB1 at the tip (16 ± 4 compared with 30 ± 4% in resting cells) and an increase in the number of comets with only CLIP-170 (17 ± 4 compared with 2 ± 1% in resting cells; Fig. 3, D and E).

To better define the role of CLIP-170 in phagocytosis, we also analyzed the microtubule network in conditions where +TIPs were depleted. In cells depleted of EB1 or CLIP-170, no strong effect on the microtubule network integrity could be observed (Fig. S3, C and D). Therefore, depletion of +TIPs does not affect the microtubules network, probably because of the redundancy of the functions of these proteins.

Together, these results show that EB1 is dispensable for phagocytosis. In addition, we observed that the plus ends of microtubules were differentially decorated with EB1 and CLIP-170 in phagocytic cups as compared with other areas in the cells. This highlights a specific role for CLIP-170 during phagocytosis in macrophages that cannot be envisaged as a mere stabilization of the microtubules network. Rather, it is specific to other aspects of CLIP-170 function.

CLIP-170/115 control actin assembly during CR3-mediated phagocytosis

Because phagocytosis is strictly dependent on actin polymerization, we then set out to determine whether functional inactivation of CLIP-170 had any consequence on the formation of actin cups at the onset of phagocytosis. CR3-induced phagocytosis relies on both Arp2/3 and mDia1 actin nucleators

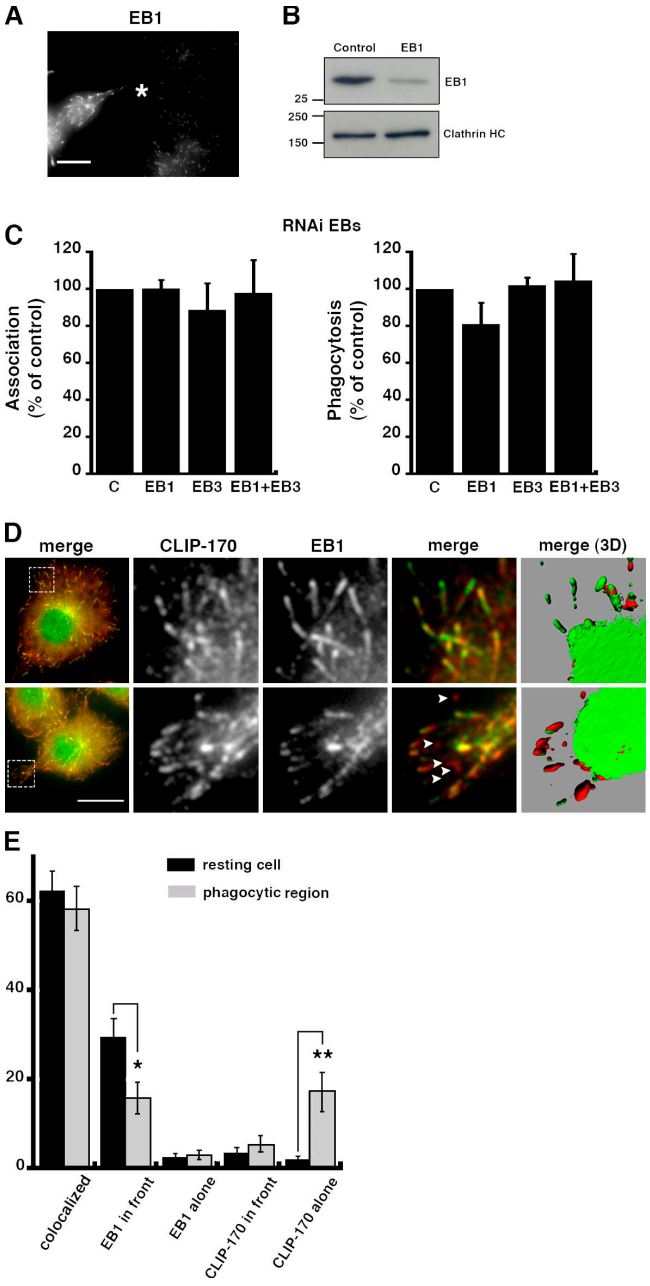

Figure 3. **EB1 is not recruited in phagocytic cups and neither EB1 nor EB3 are required for phagocytosis.** (A) RAW264.7 macrophages were transfected with siRNA directed against EB1 and after 24 h were analyzed by immunofluorescence with anti-EB1 antibodies followed by Cy3–anti-mouse IgG. Asterisk shows an EB1-depleted cell. Bar, 10 µm. (B) RAW264.7 macrophages were transfected with siRNA directed against EB1 or GFP as a control, and then lysed and analyzed by Western blotting with anti-EB1 antibodies and then with anti-clathrin as a loading control. (C) RAW264.7 macrophages were transfected with siRNA directed against EB1, EB3, or EB1 and EB3 or GFP as a control, and then allowed to phagocytose C3bi-SRBCs for 3 and 60 min. The efficiencies of association and phagocytosis were scored in 50 EB1-, EB3-, or EB1+EB3-depleted and 50 control cells (cells depleted for GFP). Results are expressed as a percentage of control cells. The means ± SEM of three independent experiments are plotted. (D) Differential recruitment of CLIP-170 and EB1 during phagocytosis. Macrophages were preactivated with PMA during 15 min (top) or preactivated and then allowed to internalize C3bi-SRBCs for 10 min (bottom). They were then analyzed by immunofluorescence with anti–CLIP-170/115 and anti-EB1 antibodies followed by Cy3–anti-rabbit IgG and Cy2–anti-mouse IgG, respectively. Bar, 10 µm. Insets show a peripheral region of a non-phagocytosing cell (top) or a phagocytosing area (bottom). Arrowheads indicate comets labeled with CLIP-170 only. 3D reconstructions of the stacks of merged images are presented in the right panels. (E) Positioning of CLIP-170/EB1 comets. Comets of CLIP-170 and EB1 were compared and the number of comets with colocalized EB1 and CLIP-170, EB1 in front of CLIP-170, EB1 alone, CLIP-170 in front of EB1, or CLIP-170 alone were counted in resting cells (black bars) and in phagocytic cups from phagocytosing cells (gray bars). Results are expressed as a percentage of the total comets counted. The means ± SEM of 586 comets (in 37 cells) from three independent experiments are plotted. *, $P < 0.05$; **, $P < 0.005$.

(May et al., 2000; Colucci-Guyon et al., 2005). We therefore also analyzed the recruitment of these two complexes at the site of phagocytosis.

For this, CLIP-170 function was impaired in RAW264.7 macrophages as in Fig. 2, which were then allowed to phagocytose C3bi-opsonized particles for 10 min before fixation (Fig. 4). We then scored the indexes of accumulation of F-actin and mDia1 at sites of phagocytosis in cells submitted to CLIP-170 inhibition (Fig. 4 A). We observed that F-actin cup formation and mDia1 recruitment were diminished in CLIP-170–depleted or –inhibited cells (Fig. 4 A). To analyze the actin cups more precisely, we also quantified the fluorescence associated with F-actin, mDia1, or Arp2/3 at sites of particle attachment and compared the signal we obtained with the signal measured in other sites of the cell (Fig. 4, B–D). We observed that F-actin, mDia1, and Arp2/3 were enriched in phagocytic cups by a factor of 2.2 ± 0.1, 1.5 ± 0.1, and 2.1 ± 0.2, respectively. We then compared the enrichments measured in CLIP-170–inhibited and control cells. To impair the function of CLIP-170, we expressed CLIP-170ΔH in RAW264.7 macrophages as described in Fig. 2. In CLIP-170–inhibited cells, the enrichment of F-actin was reduced by 35 ± 4% compared with control cells. Enrichment of mDia1 was significantly impaired (27 ± 4% reduction compared with control cells), whereas Arp2/3 recruitment was not significantly affected (12 ± 11% reduction compared with control cells; Fig. 4 D). Of note, F-actin cup formation was not impaired in cells undergoing FcR-mediated phagocytosis (90 ± 10% of control cells; Fig. S4, available at http://www.jcb.org/cgi/content/full/jcb.200807023/DC1). Functional CLIP-170 proteins are thus necessary for proper F-actin cup formation and mDia1 recruitment at sites of CR3-dependent phagocytosis.

CLIP-170 interacts with the formin homology 2 (FH2) domain of mDia1 in macrophages

To further address the cooperation between CLIP-170 and mDia1, we looked for a potential association between the two proteins. We immunoprecipitated CLIP-170 in macrophages and observed that mDia1 was coimmunoprecipitated with CLIP-170 but not in a control immunoprecipitation using a nonrelevant antibody (Fig. 5 A). We also performed immunoprecipitation of transiently expressed GFP–CLIP-170 with an anti-GFP antibody and found mDia1 coprecipitated (Fig. 5 B). We did not observe mDia1 in anti-GFP precipitates when GFP alone was expressed in macrophages. To better define the interaction between CLIP-170 and mDia1 and test whether the interaction was direct, we generated and purified GST-fused constructs of

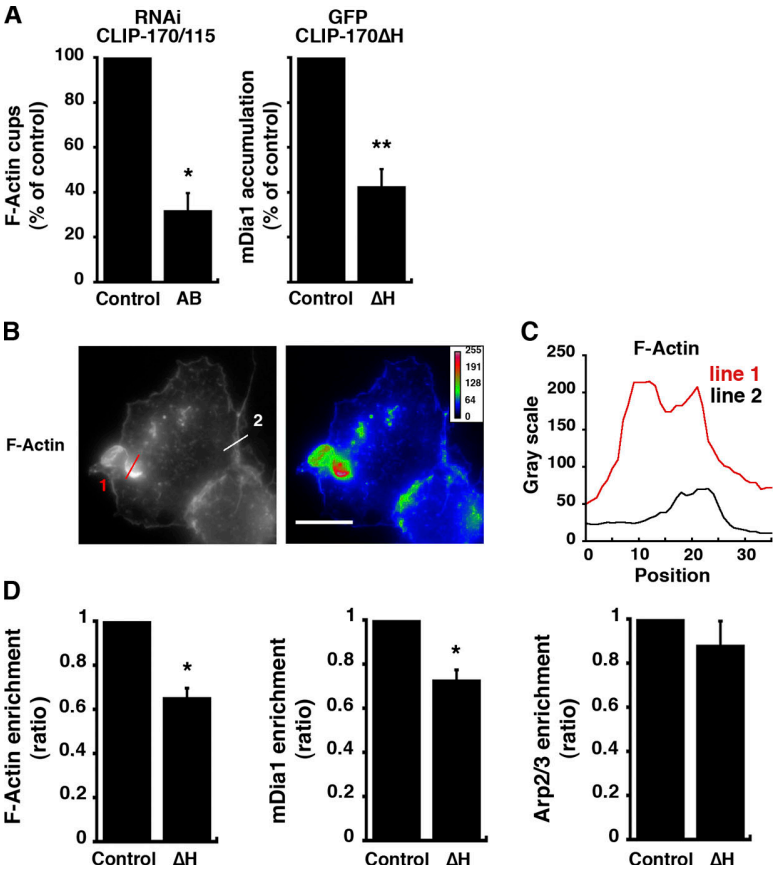

Figure 4. **CLIP-170 function is important for actin polymerization and mDia1 recruitment.** (A) RAW264.7 macrophages were transfected with pSUPER-AB (directed against CLIP-170 and CLIP-115 [left]) or pEGFP–CLIP-170ΔH (right) and then allowed to phagocytose C3bi-SRBCs for 10 min at 37°C. The cells were fixed and stained with AMCA– or Cy2–anti-rabbit IgG to detect the external particles, Alexa 488– or Alexa 350–phalloidin to stain F-actin, and anti-mDia1 or anti–CLIP-170 antibodies followed by Cy3–anti-mouse IgG. 50 CLIP-170–inhibited cells and 50 control cells were scored for the presence or absence of F-actin or mDia1 accumulation around bound particles. Results are expressed as a percentage of control cells. Means ± SEM of three independent experiments are plotted. *, $P < 0.001$; **, $P < 0.005$. (B) RAW264.7 macrophages were allowed to phagocytose C3bi-SRBCs for 10 min at 37°C, fixed, permeabilized, and incubated with Alexa 546–phalloidin. Images are shown using the Gray-scale (left) or Rainbow2 (right) look-up tables. Values on the color scales in the right corner of the right panel indicate the fluorescence intensities. Bar, 10 µm. (C) The profiles of F-actin fluorescence intensities along the line drawn at the phagocytic site (line 1) and in the cell body (line 2) are shown. (D) Macrophages were transfected with pEGFP–CLIP-170ΔH or pEGFP as a control and then phagocytosis was performed as in B. mDia1 was detected with specific antibodies and the Arp2/3 complex was stained with anti-p16 antibodies, each followed by Cy3-F(ab')$_2$ anti-mouse IgG antibodies. The fluorescence intensities measured in the phagocytic cups were background subtracted and expressed as a percentage of the intensities in the cell body. Data obtained for F-actin (left), mDia1 (middle), and Arp2/3 (right) were plotted. Data are the mean ± SEM of three independent experiments. 15 CLIP-170ΔH–expressing and 15 GFP-expressing control cells were analyzed in each experiment. *, $P < 0.005$. Enrichment of Arp2/3 was not significantly impaired ($P > 0.1$).

CLIP-170 (Scheel et al., 1999; Fig. 5 D) and tested their potential interaction with purified His-tagged mDia1 constructs (Fig. 5 C). We used purified N- or C-terminal (FH1-FH2-DAD) constructs of mDia1, as well as the FH2 domain alone (Romero et al., 2004; Copeland et al., 2007). We observed interaction between a C-terminal construct of CLIP-170 (T6) and the FH1-FH2-DAD domain of mDia1 (not depicted), but not with the N-terminal portion of the protein (Fig. 5 E). The FH2 domain of mDia1, which is the minimal domain of mDia1 with actin nucleation activity in vitro, was sufficient to interact efficiently with CLIP-170 (Fig. 5 E). Using various truncated constructs of CLIP-170, we demonstrated that neither the N-terminal domain (H1) containing Cap-Gly domains nor the C-terminal domain (T4) containing metal-binding domains exhibited a strong interaction with mDia1-FH2 (Fig. 5 F). The T6 construct that binds efficiently to mDia1-FH2 is composed of a coiled-coil region (M) and the C-terminal metal-binding domain (T4), but none of these regions were able to bind efficiently to mDia1-FH2. Therefore, the interaction between CLIP-170 and mDia1 involves a C-terminal region of CLIP-170 comprising a coiled-coil region and the metal-binding regions and the FH2 domain of mDia1. We performed pull-down experiments with various concentrations of CLIP-170–T6 to quantify the affinity of the binding between CLIP-170–T6 and mDia1-FH2. The best fit of the curve gave a K_d of 0.8 µM. We then tested whether the binding of CLIP-170–T6 to the FH2 domain of mDia1 had any effect on the in vitro actin nucleation promoted by FH2 or the FH1-FH2-DAD constructs (Fig. S5 A, available at http://www.jcb.org/cgi/content/full/jcb.200807023/DC1). We observed that GST–CLIP-170–T6 had no effect on the nucleating activity of mDia1 constructs. In addition, the CLIP-170–T6 construct did not reverse the inhibition of the nucleating activity of FH1-FH2-DAD by the N-terminal part of the mDia1 protein (Fig. S5 B). These results suggest that CLIP-170 does not regulate the actin-nucleating activity of mDia1.

CLIP-170 and mDia1 interact independently of microtubules or actin filaments and their interaction is regulated during phagocytosis

The association between endogenous CLIP-170 and mDia1 proteins was not dependent on the presence of microtubules or microfilaments in the cells because the coimmunoprecipitation was observed when cells were pretreated with the microtubule-stabilizing drug taxol, the actin-disrupting drug latrunculin A, or the microtubule-depolymerizing drug nocodazole (Fig. 6 A). In addition, actin and tubulin were not detected in the coimmunoprecipitations of CLIP-170 and mDia1 (unpublished data). This is consistent with the observation that the two recombinant proteins interacted in vitro (Fig. 5).

We then analyzed whether the interaction between CLIP-170 and mDia1 was regulated during phagocytosis. For this, RAW264.7 macrophages were induced to phagocytose opsonized particles to target CR3 or FcR for various times and then lysed on ice. CLIP-170 was immunoprecipitated and the presence of mDia1 in the precipitates was assessed by Western blotting

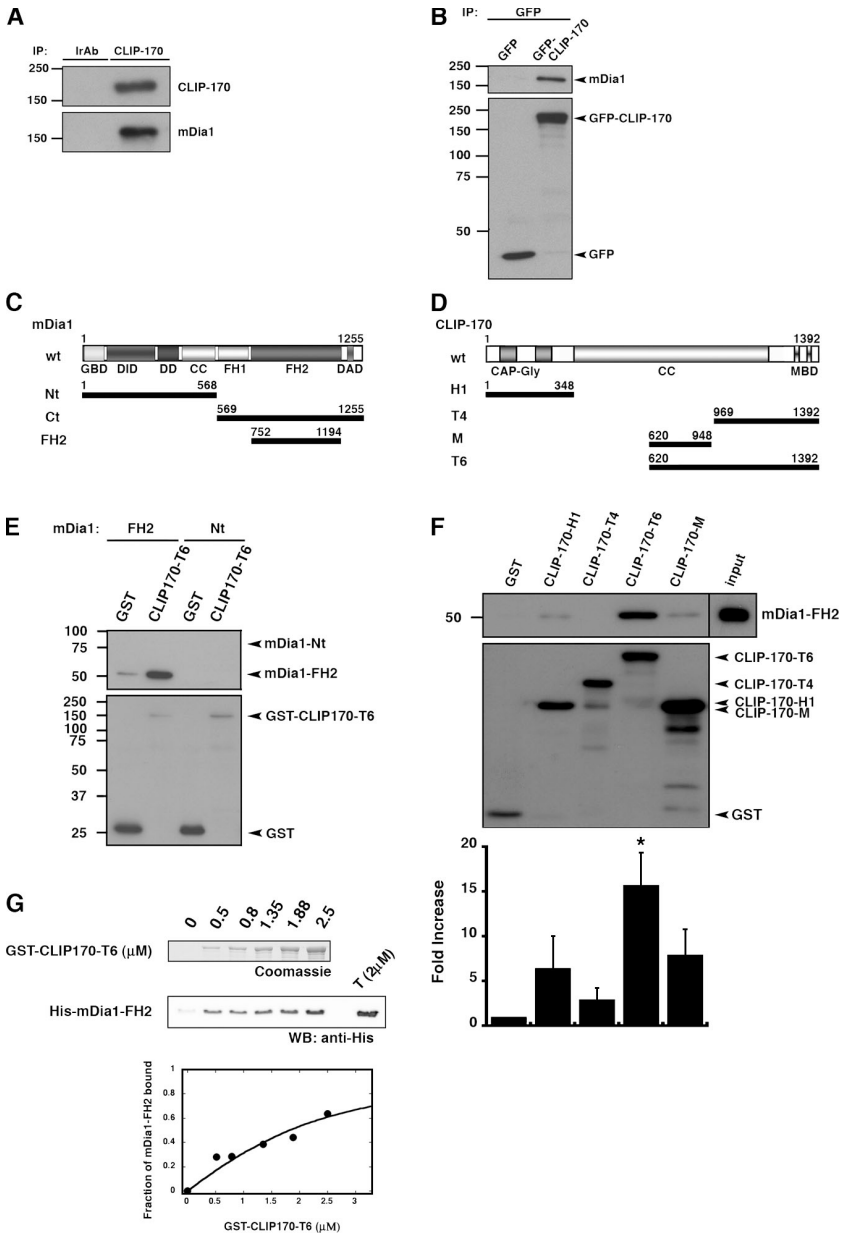

Figure 5. **CLIP-170 interacts with the FH2 domain of mDia1 directly.** (A) Endogenous mDia1 and CLIP-170 coimmunoprecipitate. RAW264.7 macrophages were lysed and immunoprecipitated with an anti–CLIP-170 antibody (clone F-3) or with an irrelevant antibody as a control (anti-myc). The samples were loaded on 7.5% SDS-PAGE and revealed by Western blotting with anti-mDia1 antibodies and after stripping with anti–CLIP-170/CLIP-115 antibodies (top). (B) GFP–CLIP-170 interacts with endogenous mDia1. HeLa cells transiently expressing GFP–CLIP-170 or GFP as a control were lysed and incubated with anti-GFP. The precipitates were analyzed for mDia1 by Western blotting. After stripping, the membranes were detected with anti-GFP antibodies (bottom). (C) Schematic representation of the His-tagged mDia1 constructs. (D) Schematic representation of the GST-fused CLIP-170 constructs. (E) CLIP-170 interacts directly with the FH2 domain of mDia1. GST or GST–CLIP-170–T6 (400 nM) bound to glutathione sepharose beads were incubated with recombinant His-tagged mDia1 constructs (500 nM). Bound material was subjected to Western blotting with anti-His antibodies and after stripping with anti-GST antibodies. The results are representative of 4–10 independent experiments with three different preparations of the GST construct, two of His-mDia1-FH2 and one of His-mDia1-Nter. (F) A C-terminal domain of CLIP-170 interacts directly with mDia1-FH2. GST or the indicated GST–CLIP-170 constructs (400 nM) bound to glutathione sepharose beads were incubated with recombinant His-FH2 (500 nM) and bound material was subjected to Western blotting with anti-His antibodies. Input represents 10% of the amount of His-FH2 added in the assay. After stripping, membranes were detected with anti-GST antibodies. The intensities of the bands were calculated using ImageJ and background subtracted. A ratio was calculated for each GST-CLIP construct as compared with GST (bottom). Results are the means ± SEM of four to eight independent experiments with three different preparations of the GST constructs. Binding of GST–CLIP-170–T6 to mDia1-FH2 was significantly higher than binding of GST (*, $P < 0.005$), whereas binding of other constructs was not ($P > 0.05$). (G) His-tagged mDia1 FH2 domain (2 μM) pull-down assays using GST–CLIP-170–T6 at the concentrations indicated. Total input (T) and bound fractions were probed with anti-His antibodies. The results were quantified to obtain the binding curve. The best fit of the curve gave a K_d of 0.8 μM.

(Fig. 6, B and C). We observed that the CLIP-170 and mDia1 interaction was not modified during FcR-mediated phagocytosis (Fig. 6 C). In contrast, a dissociation of the two proteins was observed at times as short as 1 min after the induction of phagocytosis by CR3 and was still observed 10 min later. Association started to resume 30 min after induction of CR3-dependent phagocytosis (Fig. 6 B).

These experiments thus show that CLIP-170 and mDia1 interact in macrophages independently of microtubules or actin filaments and that this interaction is negatively regulated during CR3-mediated phagocytosis. To directly visualize the localization of CLIP-170 and mDia1 in phagocytic cups, we allowed the cells to phagocytose C3bi-opsonized particles for 10 min before fixation and staining to detect simultaneously CLIP-170, mDia1, and F-actin (Fig. 6 D). We quantified the colocalization between CLIP-170 and mDia1 in phagocytic cups as compared with the rest of the cells. Using the Pearson's coefficient to evaluate colocalization (Bolte and Cordelières, 2006), we observed that CLIP-170 and mDia1 were significantly more colocalized in nonphagocytosing regions of macrophages (Pearson's coefficient 0.910 ± 0.006) than in phagocytosing regions (Pearson's coefficient 0.849 ± 0.012), although the colocalization measured was important in both cases. In addition, 3D reconstructions of the images centered on phagocytic cups showed that CLIP-170, mDia1, and F-actin are close in these structures. More precisely, in 55% of the cases, mDia1, CLIP-170, and F-actin were closely interconnected in the cups, whereas CLIP-170 was predominantly on the cytosolic side of the cup or "below" the cup in 45% of the phagocytic cups analyzed.

Together, our observations support a model in which CLIP-170, probably via microtubule binding, is important for the localization of the mDia1 actin nucleator without modifying its actin nucleation activity. Upon signaling downstream of the CR3 receptor, dissociation of CLIP-170 and mDia1 occurs, but

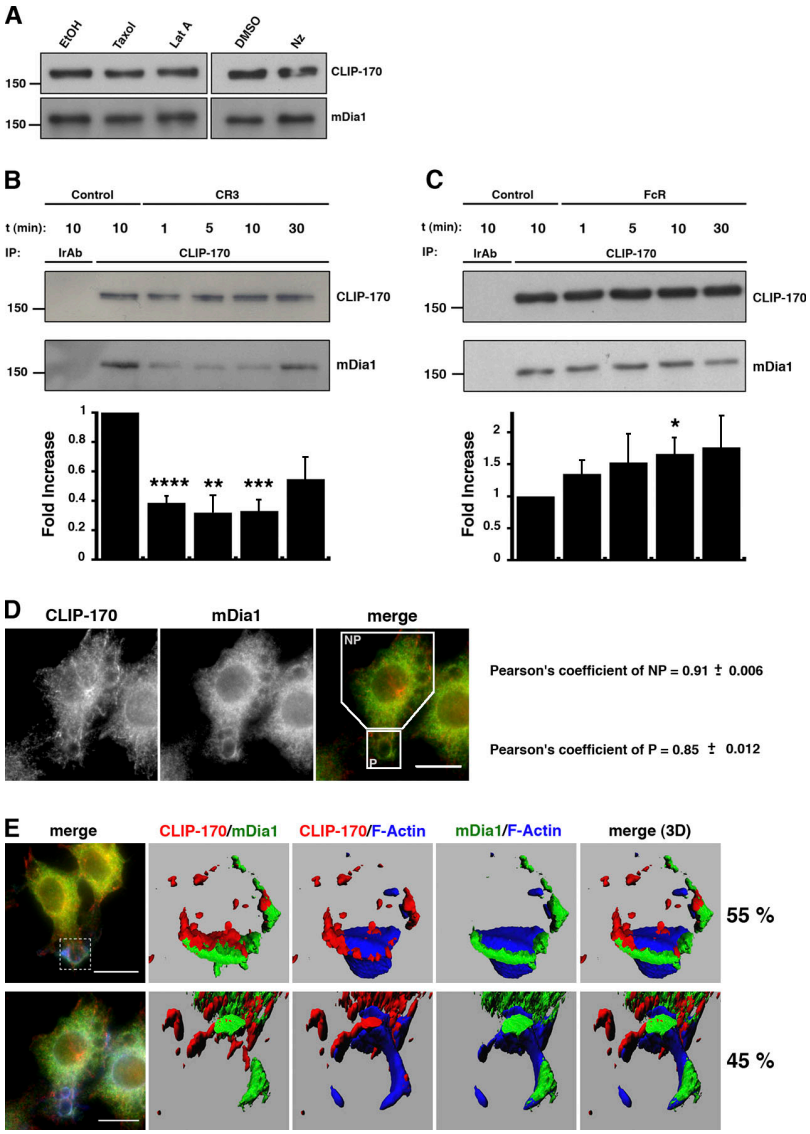

Figure 6. **CLIP-170 and mDia1 interaction does not depend on actin or microtubules and is regulated during phagocytosis.** (A) Cells were treated with 10 µM taxol, 0.1 µM latrunculin A, or 0.5 µM nocodazole during 45 min and then lysed. Lysates were analyzed as in Fig. 5 A. Data are representative of four independent experiments. (B and C) The mDia1–CLIP-170 complex is regulated during CR3- (B) but not FcR-mediated (C) phagocytosis. RAW264.7 macrophages were incubated with nonopsonized (control), C3bi-, or IgG-SRBCs for various times at 37°C. Lysates were incubated with monoclonal anti–CLIP-170 antibodies or an irrelevant antibody (IrAb). Western blots were performed using anti-mDia1 antibodies, and then with anti–CLIP-170/CLIP-115 antibodies (#2221 serum). The intensities of the bands were analyzed as in Fig. 5 F except that the ratio was calculated for each time point as compared with the control. Data are representative of three to four independent experiments. *, $P < 0.05$; **, $P < 0.005$; ***, $P < 0.001$; ****, $P < 0.0005$. (D) Recruitment of CLIP-170 and mDia1 in the phagocytic cup. Macrophages were allowed to internalize C3bi-SRBCs for 10 min. They were then fixed and analyzed by immunofluorescence with anti–CLIP-170/CLIP-115 and anti-mDia1 antibodies followed by Cy3–anti-rabbit IgG, Cy2–anti-mouse IgG, and Alexa 350–phalloidin to stain F-actin. Analysis of colocalization was performed on one plane of a stack acquired with a 0.2-µm step using the JaCop plugin of ImageJ. Colocalization was assessed with Pearson's coefficient. CLIP-170 and mDia1 were significantly more colocalized in nonphagocytosing regions of macrophages (Pearson's coefficient 0.91 ± 0.006) than in phagocytosing regions (Pearson's coefficient 0.849 ± 0.012; $P < 0.0001$). Data are representative of three independent experiments with 27 different cells in total. (E) RAW264.7 macrophages were analyzed as described in D. A z plane acquired with a 0.2-µm step is shown (left). Bar, 10 µm. Insets show a phagocytic cup presented as 3D reconstructions of the stacks of images. (top) CLIP-170, mDia1, and F-actin were closely interconnected in the phagocytic cup (55% of the cases out of 29 cells analyzed in total). (bottom) CLIP-170 was found on the cytosolic side of the cup or "below" the cup, whereas mDia1 and F-actin were intimately associated (45% of the cases out of 29 cells analyzed in total). Data are representative of three independent experiments.

both proteins remain close in the phagocytic cups and they will probably then be anchored in the cell cortex. This will allow mDia1 to play its role in F-actin polymerization.

Discussion

In this study, we show that the +TIP CLIP-170, but not EB1 or EB3, is essential for efficient phagocytosis induced by the CR3 pathway, whereas it is not involved in phagocytosis induced by FcR. We uncover a role for this microtubule-binding protein in mDia1 recruitment and in polymerization of actin induced downstream of CR3 receptors. We found that CLIP-170 interacts directly with mDia1 and that this interaction is regulated during CR3-mediated phagocytosis, highlighting a cross talk between the actin and the microtubule cytoskeleton downstream of the αMβ2/CR3 integrin receptors.

We observed that CLIP-170, which labels the plus ends of microtubules, is accumulated in phagocytic cups using both immunofluorescence and YFP-tagged proteins in living macrophages. The role of microtubules in the maturation of closed phagosomes and their movement to the cell center has been clearly established (Toyohara and Inaba, 1989; Blocker et al., 1997, 1998). Furthermore, it was suggested that association of early phagosomes with the plus ends of microtubules allows their movement by following growth or shrinkage of microtubules (Blocker et al., 1998). The role of microtubules at the onset of phagocytosis has been investigated in primary macrophages in seminal comparative studies (Kaplan, 1977; Newman et al., 1991; Allen and Aderem, 1996), which showed that the cytoskeletal structures required for complement and FcR-mediated phagocytosis are different. Indeed, CR3-mediated phagocytosis required microtubules and was less dependent on actin, whereas FcR-mediated phagocytosis was independent of the integrity of the microtubule cytoskeleton. Our own results corroborate these studies. In addition, recent data showed that CLIP-170 is crucial for enhanced spreading and FcR-mediated phagocytosis in activated macrophages even though it is dispensable for basal levels of FcR-mediated phagocytosis in resting cells (Binker et al., 2007; Khandani et al., 2007). Therefore, all these studies underline the predominant role of microtubules and now of CLIP-170

in phagocytosis in activated macrophages. Our results also support a specific requirement for CLIP-170 in CR3-mediated phagocytosis and provide novel mechanistic data on the role of CLIP-170 during phagocytosis.

Using both a dominant-negative approach and RNA interference, we showed that CLIP-170 is necessary for optimal phagocytosis induced by CR3 in macrophages. Depletion of both CLIP-170 and CLIP-115 leads to a comparable decrease in phagocytosis efficiency compared with the impact of the depletion of CLIP-170 alone. Therefore, although the two proteins contain similar microtubule-binding domains in their N-terminal region and although they were shown to interact (Hoogenraad et al., 2000; Lansbergen et al., 2004), no clear synergy between CLIP-115 and CLIP-170 was observed in macrophages during phagocytosis. This could be explained by the fact that CLIP-170 interacts with mDia1 via its unique C-terminal metal-binding region (see the following paragraph). Interestingly, we did not detect any involvement of EB1 or EB3 using RNA interference–based depletion. The fact that EB1 is not involved in internalization came as a surprise in light of recent reports describing EB1 as the +TIP that mediates the localization of CLIP-170 and $p150^{Glued}$ at the plus ends of microtubules (Komarova et al., 2005; Watson and Stephens, 2006). In our system, depletion of EB1 did not affect the plus end localization of CLIP-170. Moreover, the localization of EB1 and CLIP-170 differed in resting and in phagocytosing areas of macrophages and we observed an increase in the number of microtubule plus ends decorated only with CLIP-170 in phagocytic cups, as compared with nonphagocytic areas. Whether this is because of microtubule growth without EB1 or dissociation of EB1 in phagocytic cups is unclear, but EB1, as well as EB3, is dispensable for the phagosome formation, whereas CLIP-170 is not. This implies that CLIP-170 has additional EB1- and EB3-independent functions in macrophages during phagocytosis. Our data suggest that CLIP-170 may indeed control actin/microtubule cross talk in this system through an adaptor-like activity.

We had previously demonstrated that the formin family member mDia1 is specifically implicated in CR3-mediated phagocytosis and not in FcR-mediated uptake (Colucci-Guyon et al., 2005). We now show that CLIP-170 and mDia1 are found in the same complex, as observed by coimmunoprecipitation of the two proteins. This interaction does not rely on the presence of microfilaments or microtubules as it was still observed in the presence of latrunculin A or nocodazole. In addition, we observed a direct interaction between a CLIP-170 construct composed of a coiled-coil region (M) and the C-terminal metal-binding domains (T4) and the FH2 domain of mDia1. We calculated that the K_d of this interaction is $\sim$0.8 μM. This result has to be considered in the context of the full-length proteins and of local concentrations at the plus ends of microtubules, which might be very high. Moreover, the two proteins probably interact as part of a larger multiprotein complex (see below). The FH2 domain is sufficient for actin nucleation in vitro. mDia1 is known to be found in a closed, inactive conformation caused by intramolecular interaction involving the diaphanous inhibitory domain as well as the coiled-coil domain and the diaphanous autoregulatory domain (DAD). Binding of mDia1 to an active Rho family GTPase then leads to the opening and the activation of the protein (Wallar and Alberts, 2003; Goode and Eck, 2007; Le Clainche and Carlier, 2008). We therefore tested whether the binding of CLIP-170–T6 to FH2 had any effect on the in vitro actin nucleation promoted by FH2 or the FH1-FH2-DAD constructs. We observed no effect. In addition, CLIP-170–T6 construct did not modify the autoinhibition as mimicked in vitro by the concomitant presence of FH1-FH2-DAD and the N-terminal part of the mDia1 protein (Fig. S5). This implies that CLIP-170 might bind to mDia1 without modifying the activity of the protein and this is compatible with a role for CLIP-170 in the localization of the protein. Therefore, based on our results, we would like to propose that, after CR3 engagement, microtubules and CLIP-170 help localize mDia1 in phagocytic cups and that this molecular interaction is lost after RhoA activation and binding to mDia1. This could then allow mDia1 to induce local polymerization of actin leading to particle engulfment. Both proteins would then stay close in the cell cortex without interacting. Because FcRs do not activate RhoA, the two proteins would not dissociate upon FcR triggering and mDia1 would not be activated. What drives the recruitment of CLIP-170 in phagocytic cups downstream of the CR3 receptors is still an open question. Other studies pointed at the role of microtubule depolymerization to activate GEF-H1, a RhoA exchange factor that is involved in cytokinesis (Birkenfeld et al., 2008), and therefore microtubules might act both upstream or downstream of RhoA activation.

The complex we identified and its activity is different from the mDia1/2, APC, and EB1-containing complex that was reported in fibroblasts (Wen et al., 2004). In that case, RhoA-activated mDia1/2 binds to and stabilizes microtubules (Palazzo et al., 2001; Wen et al., 2004). Interestingly, this property was recently shown to be independent of the actin nucleation activity of mDia1 (Bartolini et al., 2008). We observed that a microtubule-stabilizing protein, CLIP-170, allows the localization and function of mDia1, thus allowing correct actin polymerization at phagocytic sites. A recent study suggested that IQGAP1 is necessary for activated Dia1 localization at the front of migrating fibroblasts and in avidin-coated beads containing phagosomes in macrophages (Brandt et al., 2007). IQGAP1 is an effector of Rac1 and Cdc42 that was found in a tripartite complex with the activated Rac1/Cdc42 and CLIP-170 in fibroblasts (Fukata et al., 2002). Because complement-mediated phagocytosis does not depend on Rac1/Cdc42 (Caron and Hall, 1998; Colucci-Guyon et al., 2005), it seems unlikely that IQGAP1 directs the recruitment of CLIP-170 during CR3 phagocytosis, although we cannot rule out the possibility that CLIP-170, mDia1, and IQGAP1 are acting together during phagocytosis. Indeed, CLIP-170 and mDia1 might be part of a multiprotein complex and this will be the focus of a future study. Several proteins have been reported recently to support cross talks between actin and microtubules in different systems and our results unravel new players for the temporally and spatially coordinated regulation of the actin and microtubule cytoskeletons. This may be important not only for phagocytosis but also for related processes such as cell spreading and migration, two functions that also require activation of integrins.

Materials and methods

Reagents

PMA (used at 150 ng/ml from a 1-mg/ml stock in DMSO), taxol (paclitaxel, used at 10 µM from a 10-mM stock in ethanol), nocodazole (used at 0.5 µM from a 10-mM stock in DMSO), latrunculin A (used at 0.1 µM from a 500-µM stock in ethanol), and complement C5-deficient serum were obtained from Sigma-Aldrich. The following antibodies were used: anti–CLIP-170 (clone F-3; Santa Cruz Biotechnology, Inc.); #2221 serum (a gift from N. Galjart, Erasmus University, Rotterdam, Netherlands); anti-EB3 serum (a gift from A. Akhmanova, Erasmus University); anti–α-tubulin (DM1A; Sigma-Aldrich); anti-myc (Roche); anti-mDia1, anti-EB1, anti-CLIP-115, and anti-clathrin heavy chain (BD); anti–p16-Arc (Synaptic Systems GmbH); anti-GST (home made); anti-tubulin (clone F2C; Nizak et al., 2003; Moutel et al., 2009); purified rabbit anti-SRBC (IGN Biochemicals); purified rabbit anti-SRBC IgM (Accurate); AMCA-, Cy2-, Cy3-, or Cy5-labeled F(ab')$_2$ anti-mouse, -human, and -rabbit (Jackson ImmunoResearch Laboratories); HRP-labeled anti-mouse and anti-rabbit IgG (Jackson ImmunoResearch Laboratories). Alexa 350/488–coupled phalloidins were obtained from Invitrogen.

Plasmids

The GFP–CLIP-170 plasmid was described in Fukata et al. (2002) and YFP–CLIP-170 was derived from this construct. GFP–CLIP-170ΔH was provided by A. Akhmanova (Komarova et al., 2002), as were the pSuper plasmids CLIP-170A (5′-GGAGAAGCAGCAGCACATT-3′), CLIP-115A (5′-GGCACAGCATGAGCAGTAT-3′), and CLIP-115B (5′-CTGGAAATCC-AAGCTGGAC-3′; Lansbergen et al., 2004). As a control, the pSUPER plasmid for giantin depletion (Miserey-Lenkei et al., 2006) was used. The pEGFP-N1 plasmid was purchased from Clontech Laboratories, Inc.

Cell culture, transfection, and siRNA treatment

RAW264.7 macrophages were grown and transfected as described previously (Niedergang et al., 2003). Transfections with siRNA duplex (Eurogentec) specific for mouse EB1 or for GFP were performed according to the manufacturer's instructions using Lipofectamine 2000 (Invitrogen; Elbashir et al., 2001). The EB1-specific siRNA sequence was 5′-AAGUGAAAUUC-CAAGCUAAGC-3′ as described previously (Wen et al., 2004). The EB3-specific siRNA sequence was 5′-ACUAUGAUGGAAAGGAUUAC-3′ as described previously (Komarova et al., 2005). siRNA duplex against GFP was described previously (Braun et al., 2004). After 24 h, cell lysates were analyzed by Western blotting or immunofluorescence as described by Braun et al. (2004).

Phagocytosis assays and quantitation

When indicated, cells were pretreated with taxol for 45 min at 37°C or with the same dilution of ethanol. Phagocytosis was performed as described previously (Niedergang et al., 2003; Braun et al., 2004). To quantitate phagocytosis, the number of internalized SRBCs was counted at 60 min in 50 cells randomly chosen on the coverslips, and the phagocytic index, i.e., the mean number of phagocytosed SRBCs per cell, was calculated. The index obtained for transfected or treated cells was divided by the index obtained for control cells and expressed as a percentage of control cells. We also counted the number of initial cell-associated SRBCs (at 3 min), calculated the association index (mean number of associated SRBCs per cell), and expressed it as a percentage of control cells. To quantify polymerized actin recruitment, we scored the presence or absence of F-actin accumulations around particles in 50 cells randomly chosen on the coverslips and calculated an accumulation index, i.e., the mean number of accumulations per cell. The index obtained for transfected or treated cells was divided by the index obtained for control cells and expressed as a percentage of control cells. The same method was used to assess mDia1 recruitment.

Fluorescence quantitation

Quantitation of fluorescence was performed using ImageJ Color Profiler software (National Institutes of Health) on selected linear regions in a merge z projection of maximum intensities of 8-bit stacks acquired as described in the previous paragraph with an inverted wide-field microscope (DMB; Leica) equipped with an oil immersion objective (100× Plan Apochromat HCX; 1.4 NA) and a cooled charge coupled device camera (MicroMAX; Princeton Instruments). Two areas of the cell were quantified: the phagocytic cup analyzed as three linear regions and the cell body analyzed as two linear regions. The maximum primary fluorescence intensities of each area were background corrected by subtracting the maximum value from a cell-free region. Ratios were obtained by dividing the maximum of fluorescence intensities in the phagocytic cups by the maximum fluorescence intensities in the cell body and were calculated for F-actin, mDia1, and Arp2/3 complex.

Immunofluorescence and wide-field imaging analysis

Immunofluorescence was performed as described previously (Braun et al., 2004) except for staining of EB1 and CLIP-170, which was adapted from Hoogenraad et al. (2000). In brief, the cells were fixed for 10 min in ethanol at −20°C, and then in 4% paraformaldehyde for 15 min at RT and permeabilized in 0.15% Triton X-100/PBS. Image acquisition and deconvolution were performed as described previously (Braun et al., 2004), except that the samples were examined under an inverted wide-field microscope (Axiovert 100M [Carl Zeiss, Inc.] or DMB) equipped with an oil immersion objective (100× Plan Apochromat HCX; 1.3 or 1.4 NA, respectively) and a cooled charge coupled device camera (ORCA ER [Hamamatsu Photonics] or MicroMAX, respectively). Z series of images were taken at 0.2-µm increments. 3D reconstructions were obtained using the IsoSurface function of Imaris 5.7 software (Bitplane AG). To quantitatively evaluate the level of colocalization, the Pearson's correlation coefficient (Manders et al., 1992) was calculated, with a value of one indicating complete positive correlation and zero indicating no correlation. All values were obtained with the plug-in JACoP (Bolte and Cordelières, 2006), developed for the image analysis software ImageJ. Each pairwise comparison was done on a z plane acquired with a 0.2-µm step and divided in two regions: a phagocytosing and a nonphagocytosing region.

Live-cell imaging and tracking analysis of CLIP-170–positive comets

Images were acquired every second using an inverted wide-field microscope (Axiovert 200M; Carl Zeiss, Inc.) equipped with an oil immersion objective (100× Plan Apochromat HCX; 1.4 NA*)* and a cooled charge coupled device camera (CoolSNAP HQ; Photometrics). Comet tracking was performed using the tracking function of Imaris 5.7 software. The tracks were followed for comets having a diameter >0.5 µm and appearing on five consecutive sections (gap of 1 and sort duration of 5 × t). The speed of the comets was calculated using the track speed average function.

We calculated the number of CLIP-170–positive comets per surface unit (comet index) by dividing the total number of comets during the duration of the movie calculated without sort by the mean surface of the selected area in a squared micrometer. The ratio between phagocytosing and nonphagocytosing area was obtained by dividing the comet index in the phagocytosing area by the comet index in the nonphagocytosing area for the same cell.

Coimmunoprecipitation of mDia1 with CLIP-170 in RAW264.7 cells

12–16 million RAW264.7 or HeLa cells grown to subconfluence were used for each immunoprecipitation. Cells were scraped or trypsinated and resuspended in culture medium without serum. Cells were centrifuged at 13,000 *g* for 15 s, the supernatant was removed, and cells were lysed on ice in lysis buffer (20 mM Tris, pH 7.5, 100 mM NaCl, and 0.5% NP-40) supplemented with protease inhibitors (complete EDTA-free; Roche), 1 mM sodium orthovanadate, and 50 mM NaF. The lysate was centrifuged at 13,000 *g* for 10 min at 4°C. An aliquot of the supernatant was kept to assess the amount of protein in the total lysate. After a preclearing step with protein G–Sepharose (GE Healthcare), the supernatant was incubated rotating with 1 µg of antibody and protein G–Sepharose at 4°C for 3 h and 30 min. The beads were then washed four times at 4°C in lysis buffer and once in PBS1×. The samples were analyzed by SDS-PAGE on a 7.5% gel in reducing conditions and transferred overnight onto polyvinylidene fluoride membranes (Millipore). Immunoblot was performed and revealed using ECL or ECL Plus according to the manufacturer's instructions (GE Healthcare). Stripping of membranes was performed by two subsequent incubations in 0.2 M glycine for 5 min at RT. Films were scanned and analyzed with Photoshop CS (Adobe).

When indicated, phagocytosis was performed in suspension before cell lysis. It was initiated by the addition of C3bi- or IgG-coupled SRBC in prewarmed phagocytosis medium (SRBC/macrophages ratio of 10) and synchronized by centrifugation in a microfuge (Eppendorf). After incubation at 37°C for different time points, cells were lysed and analyzed as described above.

Recombinant protein generation, purification, and pull-down assays

The GST-tagged CLIP-170 constructs were obtained either by subcloning described His-tagged constructs (Scheel et al., 1999) into pGEX4T1 (constructs H1 and T4) or by amplification of domains by PCR and cloning into pGEX2T

(constructs H3, T6, and M). For this, pET19b–CLIP-170–H1 and pET19b–CLIP-170–T4 (Scheel et al., 1999) were digested with NdeI, followed by blunting with DNA polymerase, digested with EcoRI and cloned into pGEX4T1 that was digested with BamHI, blunted with DNA polymerase, and then digested with EcoRI. CLIP-170 domains H3, T6, and M were generated by PCR using the following primers: H3, forward, 5′-CGCGGATCCATGAGTATGCTAAAGCC-3′; reverse, 5′-GGCGAATTCCCTTCTTCGGAGCTCAGC-3′; T6, forward, 5′-CGCGGATCCATGAGACTAGATTACC-3′; reverse, 5′-GGCGAATTCGAAGGTTTCGTCGTCATTG-3′; M, forward, same as T6 forward; reverse, 5′-GGCGAATTCTAGCTGCTTCTTGCTGGC-3′. They were then digested with BamHI and EcoRI and cloned into pGEX2T. The His-tagged N-terminal domain of mDia1 (amino acids 1–568) was constructed by PCR using the primers 5′-CCGGTAACATATGATGGAGCCGTCCGGCGG-3′ (forward) and 5′-GGGAATCCCTCGAGACTGCTAGAAACAGAAG-3′ (reverse), and then digested with NdeI and XhoI and cloned into pET28a(+) digested with NdeI and XhoI. His-tagged FH2 and FH1-FH2-DAD have been described previously (Romero et al., 2004).

All plasmids were transformed in *Escherichia coli* XL1blue and sequenced. All constructs were then expressed in *E. coli* BL21 and checked for protein induction by SDS-PAGE and Coomassie blue staining. Protein purification was performed after induction using 0.5 mM IPTG. Bacteria were lysed in 50 mM Tris, pH 7.5, 100 mM NaCl, 10% glycerol, 2 mM DTT, protease inhibitors (Complete Protease Inhibitor Cocktail; Roche), 0.5 mg/ml lysozyme or 50 mM Tris, pH 7.5, 500 mM NaCl, 2 mM $MgCl_2$, 1 mM DTT, and 1% Triton X-100. After clearing the bacterial lysate by centrifugation at 42,500 *g* for 30 min at 4°C, GST fusion proteins were bound to glutathione sepharose beads (GE Healthcare) and then eluted with 20 mM Tris, pH 7.5, 100 mM NaC, 2 mM β-mercaptoethanol, and 50 mM glutathion. Purified proteins were dialyzed in 20 mM Tris, pH 7.8, 100 mM NaCl, and 2 mM β-mercaptoethanol. Polyhistidine-tagged proteins were prepared as described in Romero et al. (2004). Purified proteins were separated by SDS-PAGE and quantified by comparison with bovine serum albumin using the BCA Protein Assay kit (Thermo Fisher Scientific).

GST pull-downs were performed by incubating 400 nM of GST fusion proteins with glutathione sepharose beads (8-µl bed volume) with 500 nM of His-tagged mDia1 constructs in 50 mM Tris, pH 7.5, 200 mM NaCl, 1 mM EDTA, 0.1% Tween 20, and protease inhibitors (Complete Protease Inhibitor Cocktail) for 1 h at 4°C. After three washes in the binding buffer, bound material was analyzed by Western blotting using an anti-His antibody.

To measure the equilibrium dissociation constant, increasing concentrations of GST-tagged CLIP-170–T6 bound to glutathione sepharose were incubated in the presence of 2 µM of His-tagged mDia1-FH2. The bound His-tagged mDia1-FH2 was detected by Western blotting using an anti-His tag antibody (Santa Cruz Biotechnology, Inc.) and quantified using ImageJ. The His-tagged mDia1-FH2–bound fraction was plotted as a function of total GST–CLIP-170–T6 and the following equation was used to fit the data using Kaleidagraph. The fraction R of mDia1-FH2 bound to CLIP-170–T6 is $R = \{H0 + C0 + K - [(H0 + C0 + K)^2 - 4H0 \times C0]\ 0.5\}/2H0$, where H0 is the concentration of His-tagged mDia1-FH2, C0 is the initial concentration of GST-tagged CLIP-170–T6, and K is the equilibrium dissociation constant (K_d).

Polymerization assays

Actin polymerization was monitored by the increase in fluorescence of 10% pyrenyl-labeled actin. Actin polymerization was induced by addition of 100 mM KCl, 1 mM $MgCl_2$, and 0.2 mM EGTA to a solution of Ca–ATP–G-actin containing the desired proteins. Fluorescence measurements were performed at 25°C in a spectrophotometer (Safas; Monaco).

Statistics

The statistical significance of the data were tested with an unpaired Student's *t* test, and the calculated goodness-of-fit value (p-value) is indicated in the figure legends.

Online supplemental material

Fig. S1 shows that microtubule dynamics are necessary for CR3- but not FcR-mediated or zymosan phagocytosis. Fig. S2 shows that functional CLIP-170 is not required for FcR-mediated phagocytosis. Fig. S3 shows that EB1 siRNA does not impair the +TIP localization of CLIP-170/115. Fig. S4 shows that CLIP-170 function is not important for actin polymerization and mDia1 recruitment during FcR-mediated phagocytosis. Fig. S5 shows that CLIP-170–T6 does not affect the nucleation of actin by mDia1. Online supplemental material is available at http://www.jcb.org/cgi/content/full/jcb.200807023/DC1.

We are grateful to Dr. Niels Galjart and Dr. Anna Akhmanova for the kind gift of reagents. We thank Dr. Niels Galjart for expert advice and Dr. Alexandre Benmerah for stimulating discussions. We acknowledge the contribution of Dr. Emma Colucci-Guyon to preliminary experiments. We thank Jean-François Alkombre and his team (Institut National de la Recherche Agronomique, Centre de Jouy-en-Josas) for collecting samples of sheep blood. We thank Nandi Simpson for manuscript proofreading.

This work was supported by grants from the Fondation pour la Recherche Médicale (FRM; INE20041102865), Centre National de la Recherche Scientifique (CNRS; Action Thématique et Incitative sur Programme), and Ville de Paris to F. Niedergang and from CNRS and Institut Curie to F. Perez. E. Lewkowicz was supported by a "Bourse de Docteur Ingénieur" from CNRS and a fellowship from FRM.

Submitted: 4 July 2008
Accepted: 24 November 2008

References

Aderem, A., and D.M. Underhill. 1999. Mechanisms of phagocytosis in macrophages. *Annu. Rev. Immunol.* 17:593–623.

Akhmanova, A., and M.O. Steinmetz. 2008. Tracking the ends: a dynamic protein network controls the fate of microtubule tips. *Nat. Rev. Mol. Cell Biol.* 9:309–322.

Allen, L.A., and A. Aderem. 1996. Molecular definition of distinct cytoskeletal structures involved in complement- and Fc receptor–mediated phagocytosis in macrophages. *J. Exp. Med.* 184:627–637.

Araki, N., T. Hatae, A. Furukawa, and J.A. Swanson. 2003. Phosphoinositide-3-kinase-independent contractile activities associated with Fcgamma-receptor-mediated phagocytosis and macropinocytosis in macrophages. *J. Cell Sci.* 116:247–257.

Bartolini, F., J.B. Moseley, J. Schmoranzer, L. Cassimeris, B.L. Goode, and G.G. Gundersen. 2008. The formin mDia2 stabilizes microtubules independently of its actin nucleation activity. *J. Cell Biol.* 181:523–536.

Binker, M.G., D.Y. Zhao, S.J. Pang, and R.E. Harrison. 2007. Cytoplasmic linker protein-170 enhances spreading and phagocytosis in activated macrophages by stabilizing microtubules. *J. Immunol.* 179:3780–3791.

Birkenfeld, J., P. Nalbant, S.-H. Yoon, and G.M. Bokoch. 2008. Cellular functions of GEF-H1, a microtubule-regulated Rho-GEF: is altered GEF-H1 activity a crucial determinant of disease pathogenesis? *Trends Cell Biol.* 18:210–219.

Blocker, A., F.F. Severin, J.K. Burkhardt, J.B. Bingham, H. Yu, J.C. Olivo, T.A. Schroer, A.A. Hyman, and G. Griffiths. 1997. Molecular requirements for bi-directional movement of phagosomes along microtubules. *J. Cell Biol.* 137:113–129.

Blocker, A., G. Griffiths, J.C. Olivo, A.A. Hyman, and F.F. Severin. 1998. A role for microtubule dynamics in phagosome movement. *J. Cell Sci.* 111:303–312.

Bolte, S., and F. Cordelières. 2006. A guided tour into subcellular colocalization analysis in light microscopy. *J. Microsc.* 224:213–232.

Brandt, D.T., S. Marion, G. Griffiths, T. Watanabe, K. Kaibuchi, and R. Grosse. 2007. Dia1 and IQGAP1 interact in cell migration and phagocytic cup formation. *J. Cell Biol.* 178:193–200.

Braun, V., V. Fraisier, G. Raposo, I. Hurbain, J.B. Sibarita, P. Chavrier, T. Galli, and F. Niedergang. 2004. TI-VAMP/VAMP7 is required for optimal phagocytosis of opsonised particles in macrophages. *EMBO J.* 23:4166–4176.

Caron, E. 2003. Cellular functions of the Rap1 GTP-binding protein: a pattern emerges. *J. Cell Sci.* 116:435–440.

Caron, E., and A. Hall. 1998. Identification of two distinct mechanisms of phagocytosis controlled by different rho GTPases. *Science.* 282:1717–1721.

Colucci-Guyon, E., F. Niedergang, B.J. Wallar, J. Peng, A.S. Alberts, and P. Chavrier. 2005. A role for mammalian diaphanous-related formins in complement receptor (CR3)-mediated phagocytosis in macrophages. *Curr. Biol.* 15:2007–2012.

Copeland, S.J., B.J. Green, S. Burchat, G.A. Papalia, D. Banner, and J.W. Copeland. 2007. The diaphanous inhibitory domain/diaphanous autoregulatory domain interaction is able to mediate heterodimerization between mDia1 and mDia2. *J. Biol. Chem.* 282:30120–30130.

Coppolino, M.G., R. Dierckman, J. Loijens, R.F. Collins, M. Pouladi, J. Jongstra-Bilen, A.D. Schreiber, W.S. Trimble, R. Anderson, and S. Grinstein. 2002. Inhibition of phosphatidylinositol-4-phosphate 5-kinase Iα impairs localized actin remodeling and suppresses phagocytosis. *J. Biol. Chem.* 277:43849–43857.

De Zeeuw, C.I., C.C. Hoogenraad, E. Goedknegt, E. Hertzberg, A. Neubauer, F. Grosveld, and N. Galjart. 1997. CLIP-115, a novel brain-specific

cytoplasmic linker protein, mediates the localization of dendritic lamellar bodies. *Neuron.* 19:1187–1199.

Dupuy, A.G., and E. Caron. 2008. Integrin-dependent phagocytosis: spreading from microadhesion to new concepts. *J. Cell Sci.* 121:1773–1783.

Elbashir, S.M., W. Lendeckel, and T. Tuschl. 2001. RNA interference is mediated by 21- and 22-nucleotide RNAs. *Genes Dev.* 15:188–200.

Evangelista, M., S. Zigmond, and C. Boone. 2003. Formins: signaling effectors for assembly and polarization of actin filaments. *J. Cell Sci.* 116:2603–2611.

Fukata, M., T. Watanabe, J. Noritake, M. Nakagawa, M. Yamaga, S. Kuroda, Y. Matsuura, A. Iwamatsu, F. Perez, and K. Kaibuchi. 2002. Rac1 and Cdc42 capture microtubules through IQGAP1 and CLIP-170. *Cell.* 109:873–885.

Galjart, N. 2005. CLIPs and CLASPs and cellular dynamics. *Nat. Rev. Mol. Cell Biol.* 6:487–498.

Galjart, N., and F. Perez. 2003. A plus-end raft to control microtubule dynamics and function. *Curr. Opin. Cell Biol.* 15:48–53.

Goode, B.L., and M.J. Eck. 2007. Mechanism and function of formins in the control of actin assembly. *Annu. Rev. Biochem.* 76:593–627.

Harrison, R.E., and S. Grinstein. 2002. Phagocytosis and the microtubule cytoskeleton. *Biochem. Cell Biol.* 80:509–515.

Henry, R.M., A.D. Hoppe, N. Joshi, and J.A. Swanson. 2004. The uniformity of phagosome maturation in macrophages. *J. Cell Biol.* 164:185–194.

Hoogenraad, C.C., A. Akhmanova, F. Grosveld, C.I. De Zeeuw, and N. Galjart. 2000. Functional analysis of CLIP-115 and its binding to microtubules. *J. Cell Sci.* 113(Pt 12):2285–2297.

Howard, J., and A.A. Hyman. 2003. Dynamics and mechanics of the microtubule plus end. *Nature.* 422:753–758.

Kaplan, G. 1977. Differences in the mode of phagocytosis with Fc and C3 receptors in macrophages. *Scand. J. Immunol.* 6:797–807.

Karsenti, E., F. Nedelec, and T. Surrey. 2006. Modelling microtubule patterns. *Nat. Cell Biol.* 8:1204–1211.

Khandani, A., E. Eng, J. Jongstra-Bilen, A.D. Schreiber, D. Douda, P. Samavarchi-Tehrani, and R.E. Harrison. 2007. Microtubules regulate PI-3K activity and recruitment to the phagocytic cup during Fc{gamma} receptor-mediated phagocytosis in nonelicited macrophages. *J. Leukoc. Biol.* 82:417–428.

Komarova, Y.A., A.S. Akhmanova, S. Kojima, N. Galjart, and G.G. Borisy. 2002. Cytoplasmic linker proteins promote microtubule rescue in vivo. *J. Cell Biol.* 159:589–599.

Komarova, Y., G. Lansbergen, N. Galjart, F. Grosveld, G.G. Borisy, and A. Akhmanova. 2005. EB1 and EB3 control CLIP dissociation from the ends of growing microtubules. *Mol. Biol. Cell.* 16:5334–5345.

Lansbergen, G., and A. Akhmanova. 2006. Microtubule plus end: a hub of cellular activities. *Traffic.* 7:499–507.

Lansbergen, G., Y. Komarova, M. Modesti, C. Wyman, C.C. Hoogenraad, H.V. Goodson, R.P. Lemaitre, D.N. Drechsel, E. van Munster, T.W. Gadella Jr., et al. 2004. Conformational changes in CLIP-170 regulate its binding to microtubules and dynactin localization. *J. Cell Biol.* 166:1003–1014.

Le Clainche, C., and M.F. Carlier. 2008. Regulation of actin assembly associated with protrusion and adhesion in cell migration. *Physiol. Rev.* 88:489–513.

Lim, J., A. Wiedemann, G. Tzircotis, S.J. Monkley, D.R. Critchley, and E. Caron. 2007. An essential role for talin during alpha(M)beta(2)-mediated phagocytosis. *Mol. Biol. Cell.* 18:976–985.

Manders, E.M., J. Stap, G. Brakenhoff, R. van Driel, and J. Aten. 1992. Dynamics of three-dimensional replication patterns during the S-phase, analysed by double labelling of DNA and confocal microscopy. *J. Cell Sci.* 103:857–862.

May, R.C., E. Caron, A. Hall, and L.M. Machesky. 2000. Involvement of the Arp2/3 complex in phagocytosis mediated by FcgammaR or CR3. *Nat. Cell Biol.* 2:246–248.

Miserey-Lenkei, S., A. Couedel-Courteille, E. Del Nery, S. Bardin, M. Piel, V. Racine, J.B. Sibarita, F. Perez, M. Bornens, and B. Goud. 2006. A role for the Rab6A' GTPase in the inactivation of the Mad2-spindle checkpoint. *EMBO J.* 25:278–289.

Mitchison, T., and M. Kirschner. 1984. Dynamic instability of microtubule growth. *Nature.* 312:237–242.

Moutel, S., O. Vielemeyer, H. Jin, S. Divoux, P. Benaroch, and F. Perez. 2009. Fully in vitro selection of recombinant antibodies. *Biotechnol. J.* In press.

Newman, S.L., L.K. Mikus, and M.A. Tucci. 1991. Differential requirements for cellular cytoskeleton in human macrophage complement receptor- and Fc receptor-mediated phagocytosis. *J. Immunol.* 146:967–974.

Niedergang, F., and P. Chavrier. 2005. Regulation of phagocytosis by Rho GTPases. *Curr. Top. Microbiol. Immunol.* 291:43–60.

Niedergang, F., E. Colucci-Guyon, T. Dubois, G. Raposo, and P. Chavrier. 2003. ADP ribosylation factor 6 is activated and controls membrane delivery during phagocytosis in macrophages. *J. Cell Biol.* 161:1143–1150.

Nizak, C., S. Martin-Lluesma, S. Moutel, A. Roux, T.E. Kreis, B. Goud, and F. Perez. 2003. Recombinant antibodies against subcellular fractions used to track endogenous Golgi protein dynamics in vivo. *Traffic.* 4:739–753.

Olazabal, I.M., E. Caron, R.C. May, K. Schilling, D.A. Knecht, and L.M. Machesky. 2002. Rho-kinase and myosin-II control phagocytic cup formation during CR, but not FcgammaR, phagocytosis. *Curr. Biol.* 12:1413–1418.

Palazzo, A.F., T.A. Cook, A.S. Alberts, and G.G. Gundersen. 2001. mDia mediates Rho-regulated formation and orientation of stable microtubules. *Nat. Cell Biol.* 3:723–729.

Perez, F., G.S. Diamantopoulos, R. Stalder, and T.E. Kreis. 1999. CLIP-170 highlights growing microtubule ends in vivo. *Cell.* 96:517–527.

Pierre, P., J. Scheel, J.E. Rickard, and T.E. Kreis. 1992. CLIP-170 links endocytic vesicles to microtubules. *Cell.* 70:887–900.

Romero, S., C. Le Clainche, D. Didry, C. Egile, D. Pantaloni, and M.F. Carlier. 2004. Formin is a processive motor that requires profilin to accelerate actin assembly and associated ATP hydrolysis. *Cell.* 119:419–429.

Scheel, J., P. Pierre, J.E. Rickard, G.S. Diamantopoulos, C. Valetti, F.G. van der Goot, M. Haner, U. Aebi, and T.E. Kreis. 1999. Purification and analysis of authentic CLIP-170 and recombinant fragments. *J. Biol. Chem.* 274:25883–25891.

Stuart, L.M., and R.A. Ezekowitz. 2005. Phagocytosis: elegant complexity. *Immunity.* 22:539–550.

Swanson, J.A., M.T. Johnson, K. Beningo, P. Post, M. Mooseker, and N. Araki. 1999. A contractile activity that closes phagosomes in macrophages. *J. Cell Sci.* 112(Pt 3):307–316.

Toyohara, A., and K. Inaba. 1989. Transport of phagosomes in mouse peritoneal macrophages. *J. Cell Sci.* 94(Pt 1):143–153.

Wallar, B.J., and A.S. Alberts. 2003. The formins: active scaffolds that remodel the cytoskeleton. *Trends Cell Biol.* 13:435–446.

Watson, P., and D.J. Stephens. 2006. Microtubule plus-end loading of p150(Glued) is mediated by EB1 and CLIP-170 but is not required for intracellular membrane traffic in mammalian cells. *J. Cell Sci.* 119:2758–2767.

Wen, Y., C.H. Eng, J. Schmoranzer, N. Cabrera-Poch, E.J. Morris, M. Chen, B.J. Wallar, A.S. Alberts, and G.G. Gundersen. 2004. EB1 and APC bind to mDia to stabilize microtubules downstream of Rho and promote cell migration. *Nat. Cell Biol.* 6:820–830.